Supplementary Information

(a) FM   (b) AFM
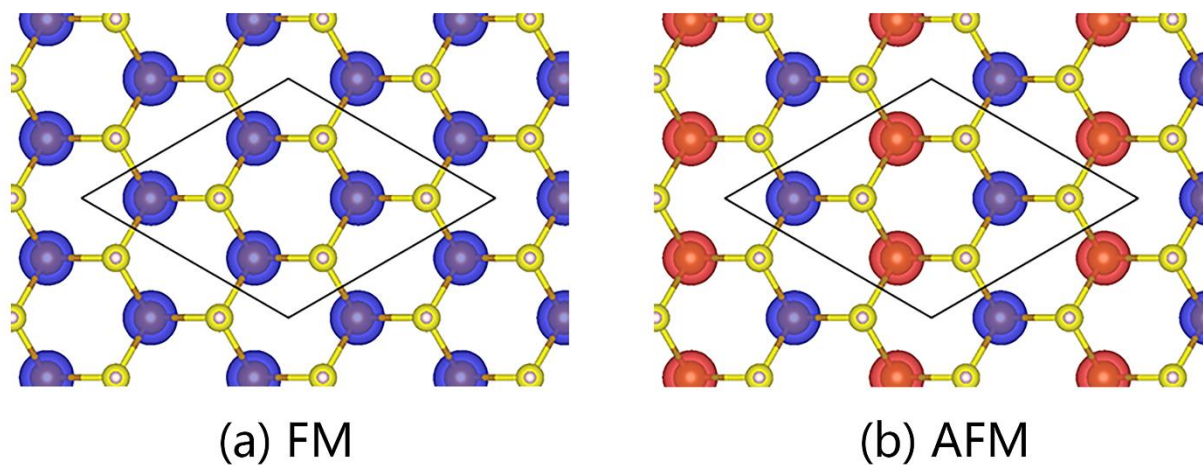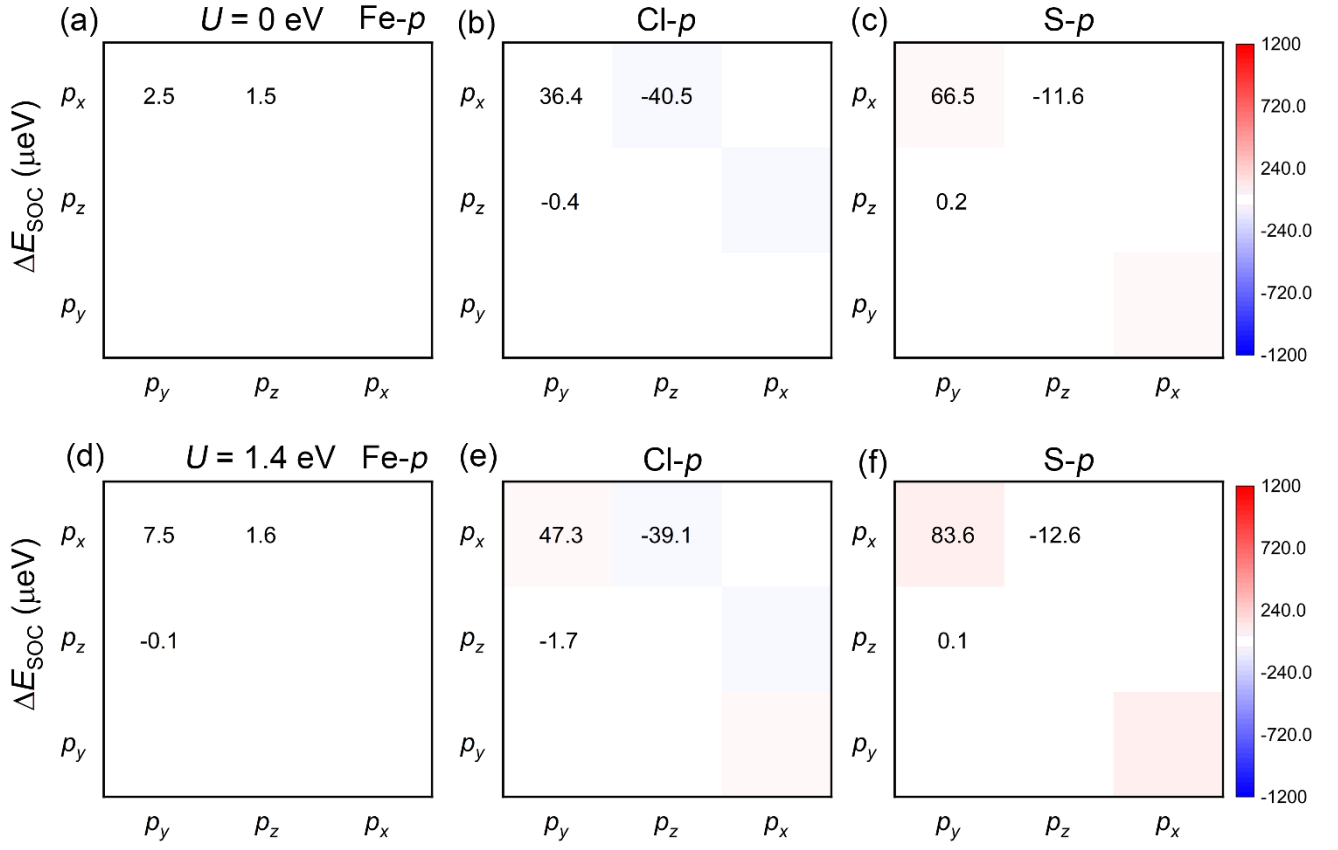
FIG. S1. Spatial distribution of spin-polarized electron density of monolayer FeClSH for (a) FM state and

(b) AFM state. Blue and red isosurfaces represent spin-up and spin-down electron density, respectively. The
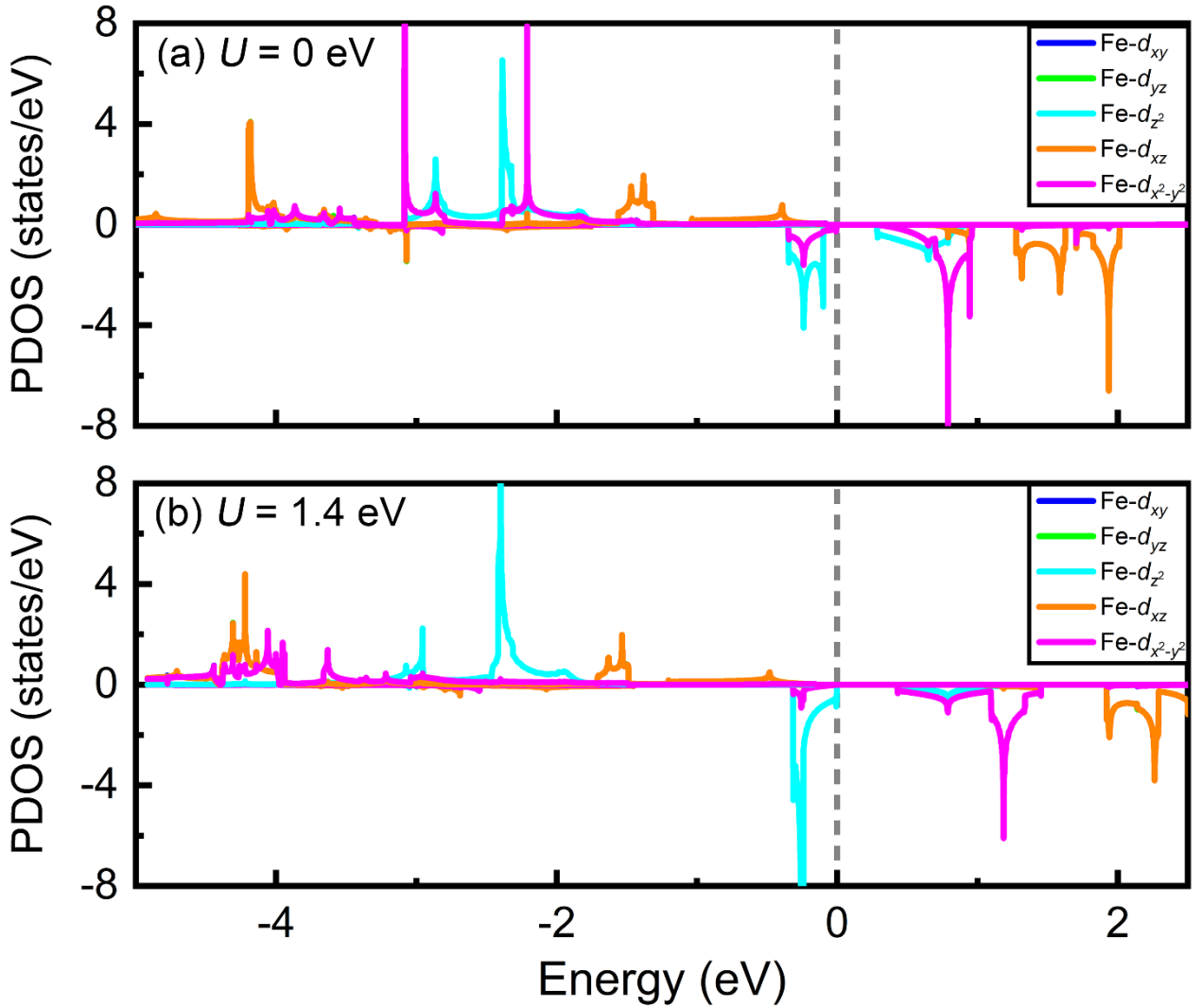
black box is a 2×2×1 supercell.

FIG. S2. Orbital-resolved ΔE_{SOC} of the monolayer FeClSH for $U = 0$ eV and 1.4 eV. (a) Fe-p orbitals, (b) Cl-p orbitals, and (c) S-p orbitals for $U = 0$ eV. (d) Fe-p orbitals, (e) Cl-p orbitals, and (f) S-p orbitals for $U = 1.4$ eV.

Table S1. Lattice constant a (Å), bond angle (°), and $E_{AFM} - E_{FM}$ (meV per unit cell) for $U = 0$ eV and 1.4 eV.

U	a	Fe-Cl-Fe	Fe-S-Fe	$E_{AFM} - E_{FM}$
0	3.51	87.5	92.7	133.79
0	3.57	88.1	93.6	117.66
1.4	3.51	87.5	92.7	27.56
1.4	3.57	88.1	93.6	14.13

Table S2. Matrix differences of $\left|\langle u,\alpha|L_z|o,\beta\rangle\right|^2 - \left|\langle u,\alpha|L_y|o,\beta\rangle\right|^2$ for Fe-d orbitals.

u^-	o^+					o^-				
	d_{xy}	d_{yz}	d_{z2}	d_{xz}	d_{x2-y2}	d_{xy}	d_{yz}	d_{z2}	d_{xz}	d_{x2-y2}
d_{xy}	0	1	0	0	-4	0	-1	0	0	4
d_{yz}	1	0	0	-1	0	-1	0	0	1	0
d_{z2}	0	0	0	3	0	0	0	0	-3	0
d_{xz}	0	-1	3	0	1	0	1	-3	0	-1
d_{x2-y2}	-4	0	0	1	0	4	0	0	-1	0

FIG. S3. PDOS of different atomic orbitals for (a) $U = 0$ eV and (b) $U = 1.4$ eV.
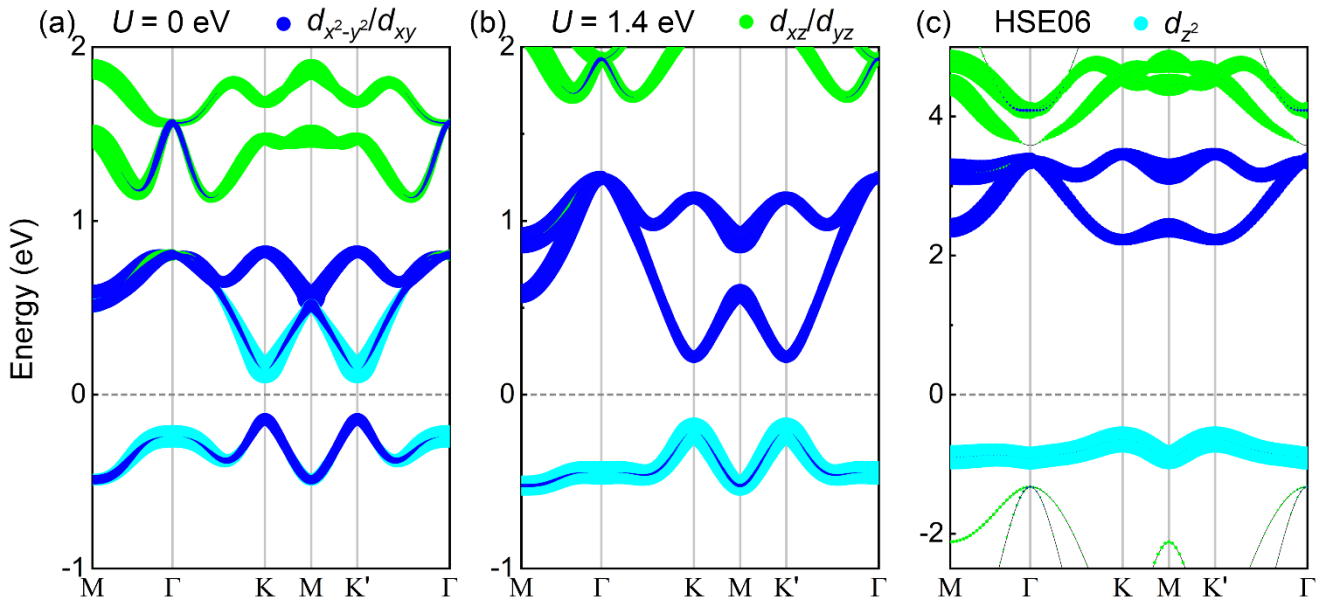
FIG. S4. Orbital-resolved band structures of spin-down without SOC for (a) $U = 0$ eV, (b) $U = 1.4$ eV, and (c) HSE06.
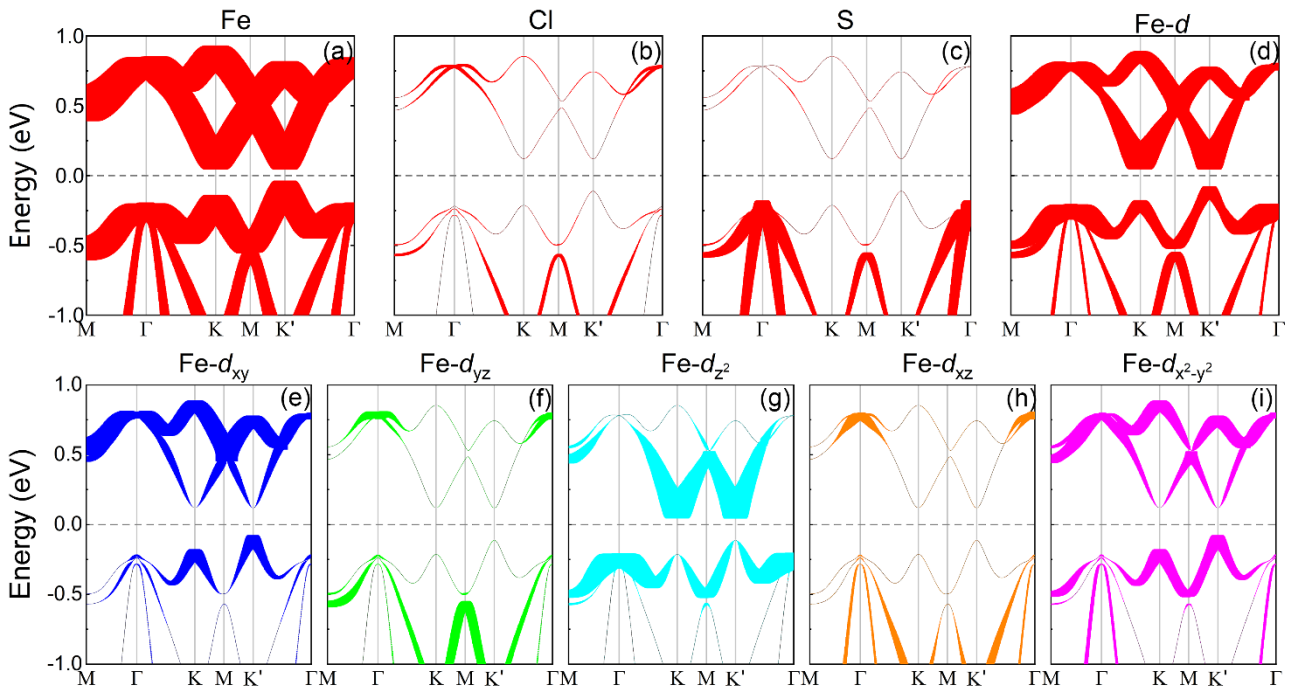
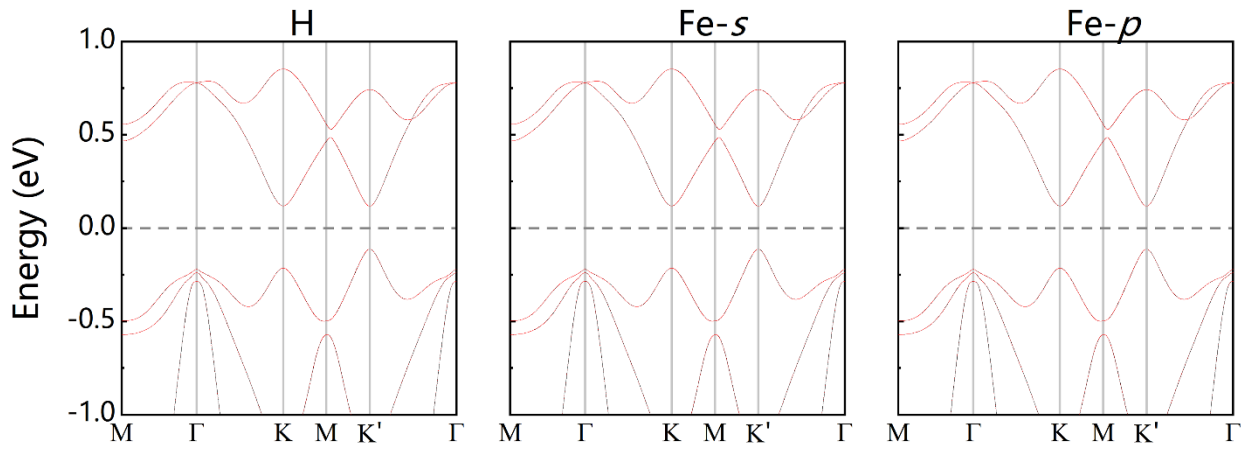**FIG. S5.** Orbital-resolved band structures with SOC for $U = 0$ eV.

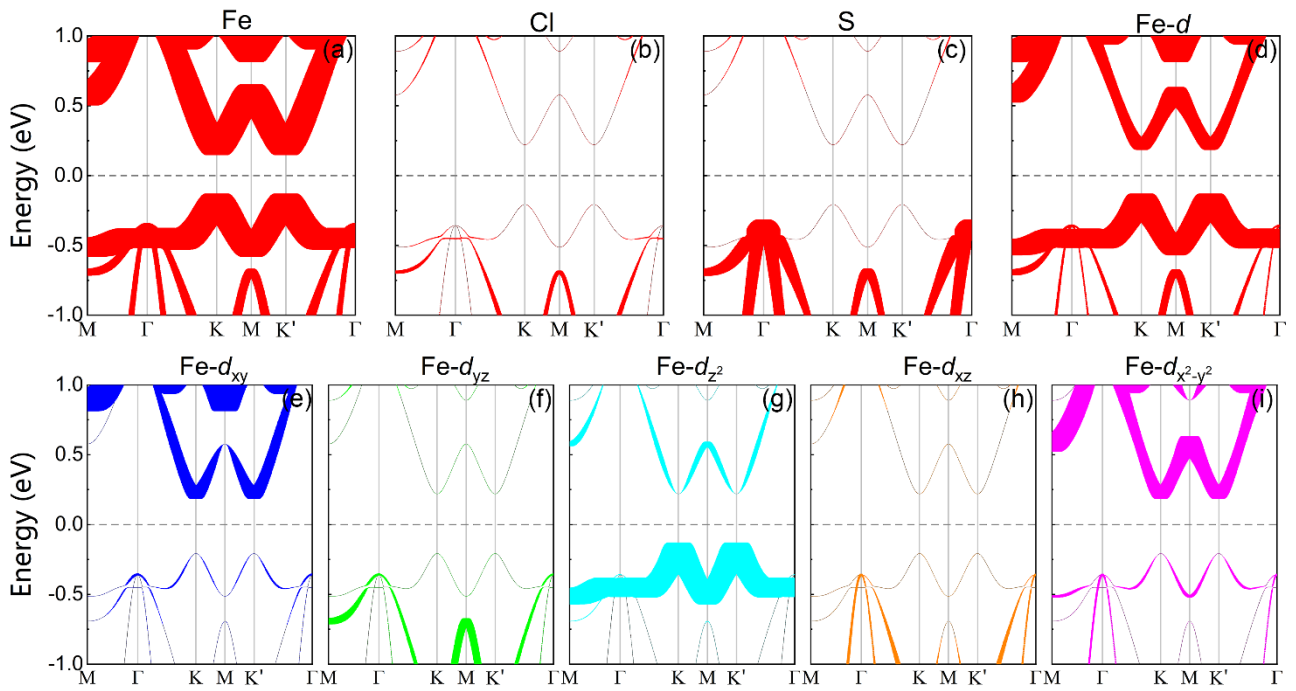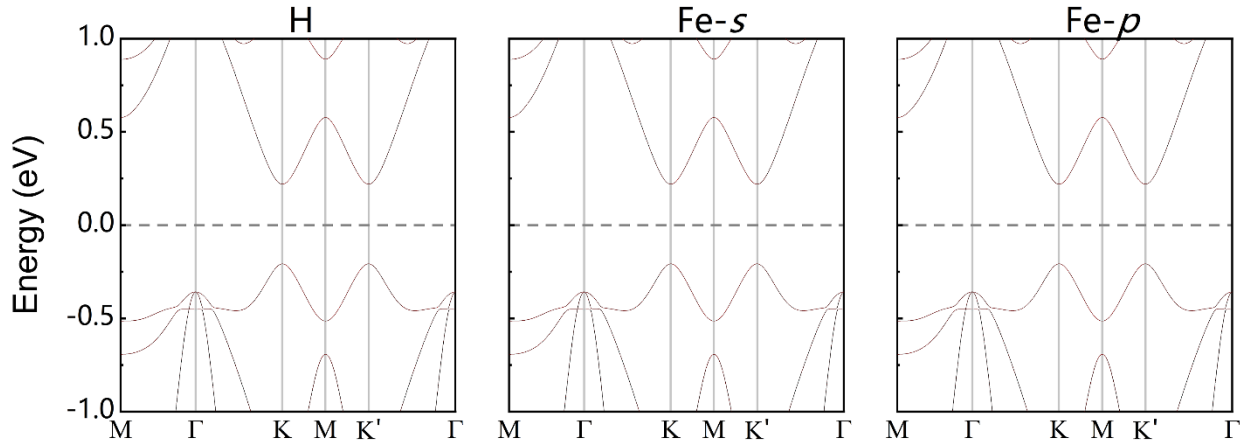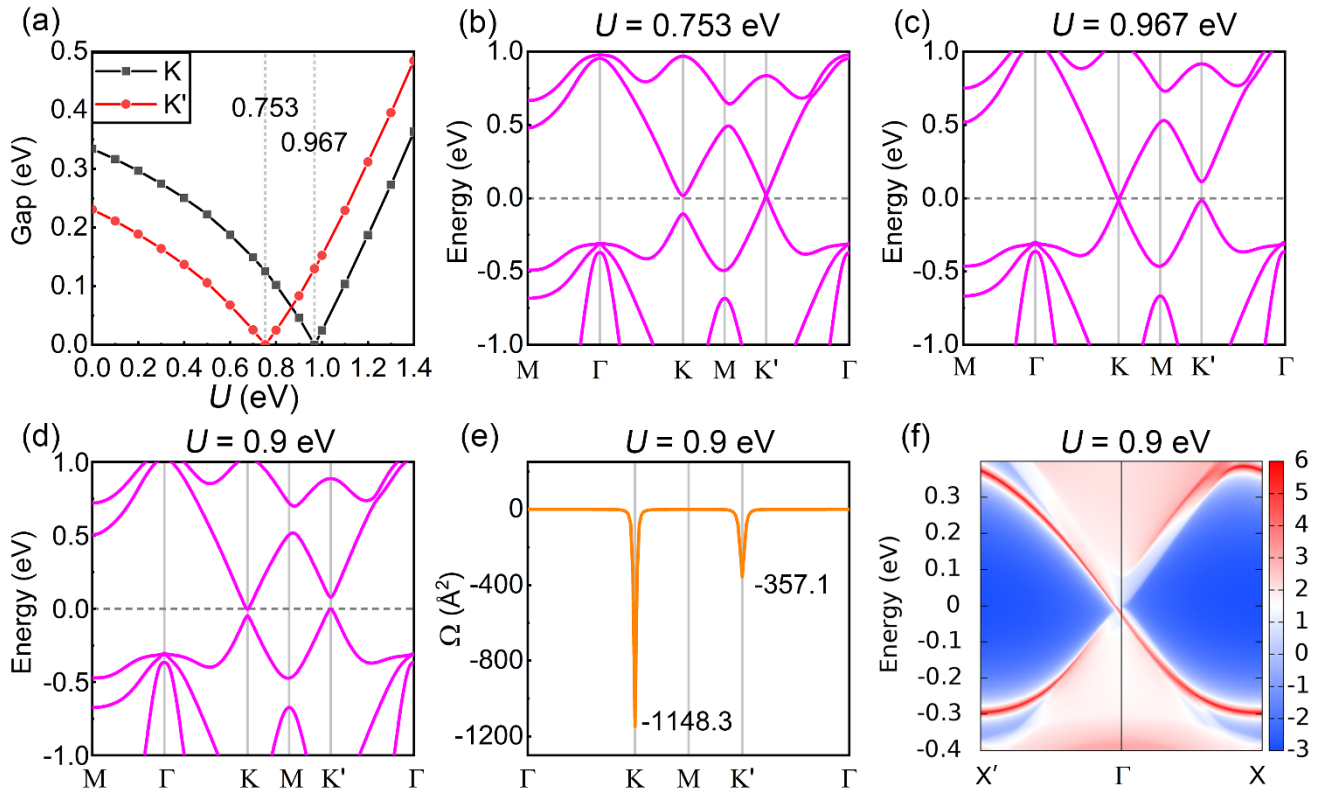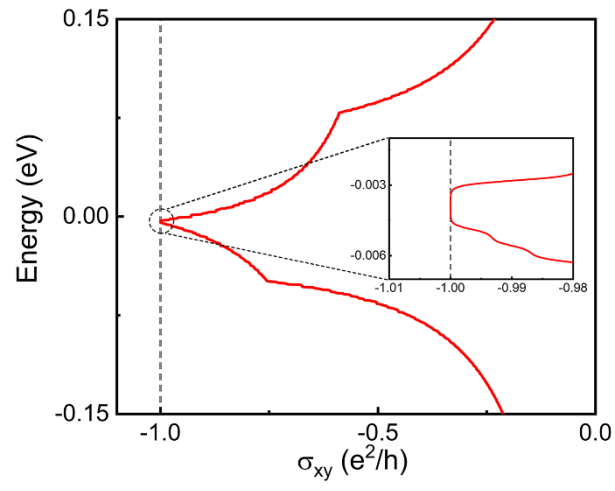**FIG. S6.** Orbital-resolved band structures with SOC for $U = 0$ eV.

FIG. S7. Orbital-resolved band structures with SOC for $U = 1.4$ eV.

FIG. S8. Orbital-resolved band structures with SOC for $U = 1.4$ eV.

FIG. S9. (a) Band gaps located at K and K' valleys and band structures for (b) $U = 0.753$ eV and (c) 0.967 eV. (d) Band structure, (e) Berry curvature, and (f) edge state for $U = 0.9$ eV.

FIG. S10. AHC for $U = 0.9$ eV.